

This work was written as part of one of the author's official duties as an Employee of the United States Government and is therefore a work of the United States Government. In accordance with 17 U.S.C. 105, no copyright protection is available for such works under U.S. Law.

Public Domain Mark 1.0

<https://creativecommons.org/publicdomain/mark/1.0/>

Access to this work was provided by the University of Maryland, Baltimore County (UMBC) ScholarWorks@UMBC digital repository on the Maryland Shared Open Access (MD-SOAR) platform.

Please provide feedback

Please support the ScholarWorks@UMBC repository by emailing scholarworks-group@umbc.edu and telling us what having access to this work means to you and why it's important to you. Thank you.

Scale Dependence of Land–Atmosphere Interactions in Wet and Dry Regions as Simulated with NU-WRF over the Southwestern and South-Central United States

YAPING ZHOU

GESTAR, Morgan State University, Baltimore, and Laboratory for Atmospheres, NASA Goddard Space Flight Center, Greenbelt, Maryland

DI WU

Science Systems and Applications, Inc., Lanham, Maryland

WILLIAM K.-M. LAU

Earth System Science Interdisciplinary Center, Joint Global Change Research Institute, University of Maryland, College Park, College Park, Maryland

WEI-KUO TAO

Laboratory for Atmospheres, NASA Goddard Space Flight Center, Greenbelt, Maryland

(Manuscript received 13 January 2016, in final form 6 April 2016)

ABSTRACT

Large-scale forcing and land–atmosphere interactions on precipitation are investigated with NASA-Unified WRF (NU-WRF) simulations during fast transitions of ENSO phases from spring to early summer of 2010 and 2011. The model is found to capture major precipitation episodes in the 3-month simulations without resorting to nudging. However, the mean intensity of the simulated precipitation is underestimated by 46% and 57% compared with the observations in dry and wet regions in the southwestern and south-central United States, respectively. Sensitivity studies show that large-scale atmospheric forcing plays a major role in producing regional precipitation. A methodology to account for moisture contributions to individual precipitation events, as well as total precipitation, is presented under the same moisture budget framework. The analysis shows that the relative contributions of local evaporation and large-scale moisture convergence depend on the dry/wet regions and are a function of temporal and spatial scales. While the ratio of local and large-scale moisture contributions vary with domain size and weather system, evaporation provides a major moisture source in the dry region and during light rain events, which leads to greater sensitivity to soil moisture in the dry region and during light rain events. The feedback of land surface processes to large-scale forcing is well simulated, as indicated by changes in atmospheric circulation and moisture convergence. Overall, the results reveal an asymmetrical response of precipitation events to soil moisture, with higher sensitivity under dry than wet conditions. Drier soil moisture tends to suppress further existing below-normal precipitation conditions via a positive soil moisture–land surface flux feedback that could worsen drought conditions in the southwestern United States.

1. Introduction

Precipitation is a critical component of the global water and energy cycle and is one of the most societally relevant aspects of the weather and climate system. The

coupling and feedback between soil moisture and precipitation have been studied extensively in the last several decades (Budyko 1974; Charney et al. 1977; Shukla and Mintz 1982; Brubaker et al. 1993; Eltahir and Bras 1994).

The direct impact of soil moisture on precipitation is based on its control on evapotranspiration, that is, a direct moisture supply to precipitation and associated water recycling (Brubaker et al. 1993; Eltahir and Bras 1994; Joussaume et al. 1984; Koster et al. 1986; Dirmeyer

Corresponding author address: Dr. Yaping Zhou, NASA Goddard Space Flight Center, 8800 Greenbelt Rd., Greenbelt, MD 20771.

E-mail: yaping.zhou-1@nasa.gov

and Brubaker 1999; Brubaker et al. 2001; Bosilovich and Schubert 2002; Bosilovich and Chern 2006). However, soil moisture can also affect many other physical processes, such as the surface albedo, vegetation, and partition of surface water and heat fluxes. These can further affect planetary boundary development and moist convection (Betts and Ball 1998; Eltahir 1998; Notaro et al. 2006; Seneviratne and Stöckli 2008; Taylor and Lebel 1998; Dirmeyer et al. 2006; Koster et al. 2004; Meng et al. 2011; Pielke et al. 1999; Santanello et al. 2011; Weaver et al. 2002; Zaitchik et al. 2007). For example, Betts and Ball (1998) proposed a positive feedback mechanism through soil moisture impacting the partition of latent and sensible heat flux into the boundary layer. Under this hypothesis, drier soil moisture reduces latent heat flux but increases sensible heat flux, resulting in higher Bowen ratio and lower moist static energy (MSE), higher boundary layer height, and lifting condensation level (LCL) that tends to inhibit the shallow convection. A similar hypothesis is proposed by Eltahir (1998) through modulation of surface net radiation flux.

In addition to the local effect, the large-scale and nonlocal effect of soil moisture has been found through the impact of large-scale circulation patterns and advection of moisture from one region to another (Shukla and Mintz 1982; Meehl 1994; Douville 2002; Rowell and Blondin 1990; Beljaars et al. 1996; Zhu et al. 2009), but the scale and mechanism for these impacts are still not well understood (Cook et al. 2006; Conil et al. 2007).

As discussed above, the soil moisture–precipitation interaction involves many complicated physical processes. The most significant coupling “hot spots” are found in transitional regions where large variations of soil moisture allow its impact on precipitation (Koster et al. 2004). The interaction could take place in two modes: a dynamic mode before and during storm events (from hours to days) and a slow mode associated with the long-term (from months to seasons) variability of precipitation, evaporation, and soil moisture (Barros and Hwu 2002). Thus, it is important to study the soil moisture–precipitation feedback under given spatial and temporal scales in any regions. In this study, we will review some of the fundamental questions in soil moisture–precipitation feedback, that is, the relative importance of large-scale forcing and soil moisture in different regions (dry and wet) and different kinds of rain events (light and heavy) under the same moisture budget framework. In particular, we will examine how the results may change with spatial and temporal scales. Here large-scale forcing refers to the large-scale atmospheric conditions such as those analyzed in section 3a and are used to drive the regional NU-WRF as initial and lateral boundary conditions. The study uses

NU-WRF simulations of two contrasting years, 2010 and 2011, focusing on spring and early summer in the southern United States. Section 2 describes model experiments and validation datasets. Section 3 analyzes the model simulation results. Section 4 provides a summary and discussion.

2. Data and methodology

a. NU-WRF

The NASA-Unified WRF (NU-WRF; <http://nuwrf.gsfc.nasa.gov>) modeling system has been developed at the Goddard Space Flight Center (GSFC) as an observation-driven integrated modeling system that represents aerosol, cloud, precipitation, and land processes at satellite-resolved scales (Peters-Lidard et al. 2015). NU-WRF is a superset of the National Center for Atmospheric Research (NCAR) Advanced Research version of WRF (ARW) dynamical core model (Skamarock and Klemp 2008), achieved by fully integrating the GSFC Land Information System (LIS; Kumar et al. 2006; Peters-Lidard et al. 2011), the WRF-Chem enabled version of the Goddard Chemistry Aerosol Radiation and Transport (GOCART; Chin et al. 2000) model, the Goddard Satellite Data Simulator Unit (G-SDSU; Matsui et al. 2014), and custom boundary/initial condition preprocessors. Several NASA physical packages have been implemented into NU-WRF, including the cloud-resolving model (CRM)-based microphysics (Tao et al. 2003; Lang et al. 2007, 2011, 2014) and radiation (Chou and Suarez 1999) schemes.

In this study, NU-WRF, version 3.4.1 (based on ARW, version 3.4.1), is employed to conduct high-resolution simulations. The model consists of 40 vertical levels and two spatial domains with 18- and 6-km grid spacing and time steps of 60 and 20 s, respectively. The Grell–Devenyi cumulus parameterization scheme (Grell and Devenyi 2002) is adopted for the outer domain, but the inner domain uses no convective parameterizations. The planetary boundary layer (PBL) parameterization employs the Mellor–Yamada–Janjić (Janjić 1994) level-2 turbulence closure model through the full range of atmospheric turbulent regimes. The Goddard broadband two-stream approach is used for the shortwave and longwave radiative flux calculations (Chou and Suarez 1999) with explicit interactions with clouds (microphysics). Both domains use the Goddard three-class ice (3ICE) scheme (Lang et al. 2011), which prognoses three types of ice hydrometeor species (i.e., cloud ice, snow, and graupel).

The LIS in the simulation not only provides physically consistent land surface initialization for the NU-WRF but also interacts with the surface layer and atmospheric

TABLE 1. Simulation cases, where “org” and “swp” represent simulations with original and swapped soil moisture, respectively.

Simulation	Large-scale forcing	Soil moisture
S10-org	2010	2010
S10-swp	2010	2011
S11-org	2011	2011
S11-swp	2011	2010

components of the NU-WRF that produce coupled water, energy, and momentum fluxes. The LSM employed in LIS for this study is the Noah LSM version 3.2 (Ek et al. 2003). It uses the same domain configuration as the NU-WRF, providing high-resolution surface initialization with high accuracy (e.g., Wu et al. 2016). The offline LIS cold started from 1 January 2007 to 19 May 2011 to spin up the land surface states to achieve equilibrium for initialization of the WRF LIS. It uses the North American Land Data Assimilation System (NLDAS) rainfall data (Xia et al. 2012) to provide hourly rainfall and the NCEP Global Data Assimilation System (GDAS) to provide atmospheric forcing input. The NCEP North American Regional Reanalysis (NARR; Mesinger et al. 2006) is used for atmospheric initial and lateral boundary conditions for NU-WRF.

b. Experiments

The study selects two distinct years, 2010 and 2011, during the spring-to-summer transition time over the contiguous United States (CONUS) to examine the effect of large-scale forcing and land–atmosphere feedback in individual precipitation events as well as total precipitation over a season. We conducted four 3-month simulations with the NU-WRF system using original and swapped soil moisture for these two years (Table 1). The combination of these simulations allows us to examine the impact of different soil moistures under the same large-scale forcing and the impact of large-scale forcings with controlled soil moisture. The experiments run from 20 March to 20 June, covering the transition period from early spring to summer with a significant evolution of soil moisture and atmospheric boundary conditions.

c. Validation datasets

Two observational precipitation datasets are used to evaluate the model simulations. One is the precipitation forcing data prepared for the NLDAS (Mitchell et al. 2004). The NLDAS precipitation forcing over CONUS is anchored to NCEP’s $1/4^\circ$ gauge-only daily precipitation analyses of Higgins et al. (2000). In NLDAS, this daily analysis is interpolated to $1/8^\circ$ and then temporally disaggregated to hourly values

by applying hourly weights derived from hourly, 4-km, radar-based (WSR-88D) precipitation fields. The latter radar-based fields are used only to derive disaggregation weights and do not change the daily total precipitation.

The other dataset used is the Tropical Rainfall Measuring Mission (TRMM) Multisatellite Precipitation Analysis (TMPA; Huffman et al. 2007). The TMPA is a satellite-based precipitation product utilizing almost all spaceborne precipitation sensors with calibration from TRMM instruments. It combines passive microwave (PMW) precipitation estimates from a variety of low-Earth-orbiting satellites and an international constellation of five geostationary satellites, providing multisatellite precipitation estimates in 3-hourly, $0.25^\circ \times 0.25^\circ$ resolution and quasi-global (50°S – 50°N) coverage. The research version used in this study (3B42) is further adjusted with gauge measurements over land.

In addition, meteorological fields from NARR are used to examine the atmosphere large-scale and boundary conditions in section 3a. The NARR model uses the high-resolution NCEP Eta model (32 km/45 layers) together with the Regional Data Assimilation System (RDAS) that assimilates precipitation along with other variables.

3. Results

a. Meteorological conditions in the springs of 2010 and 2011

El Niño–Southern Oscillation (ENSO) is the main driver of interannual variability of precipitation in the United States (Horel and Wallace 1981; Ropelewski and Halpert 1986; Barnston et al. 1999; Ting and Wang 1997) modulated by decadal-scale variability from other climate modes such as the Pacific decadal oscillation and the Arctic Oscillation/North Atlantic Oscillation (Ting and Wang 1997; Higgins et al. 2001; Wang et al. 2014). The springs of 2010 and 2011 are interesting case studies because they represent the fast (intraseasonal) transitions of ENSO phases (Kim et al. 2011). Spring of 2010 coincided with a rapid weakening of the 2009/10 El Niño, which started in May 2009, peaked in late December 2009, and terminated in the first quarter of 2010. By April 2010, the Pacific Ocean had returned to neutral and continued to cool. A La Niña condition started to develop in June 2010, strengthening through the autumn and winter. After reaching the peak around January 2011, it again started to weaken, and by May 2011 had returned to neutral conditions, but lingering La Niña-like atmospheric impacts were still felt in the global

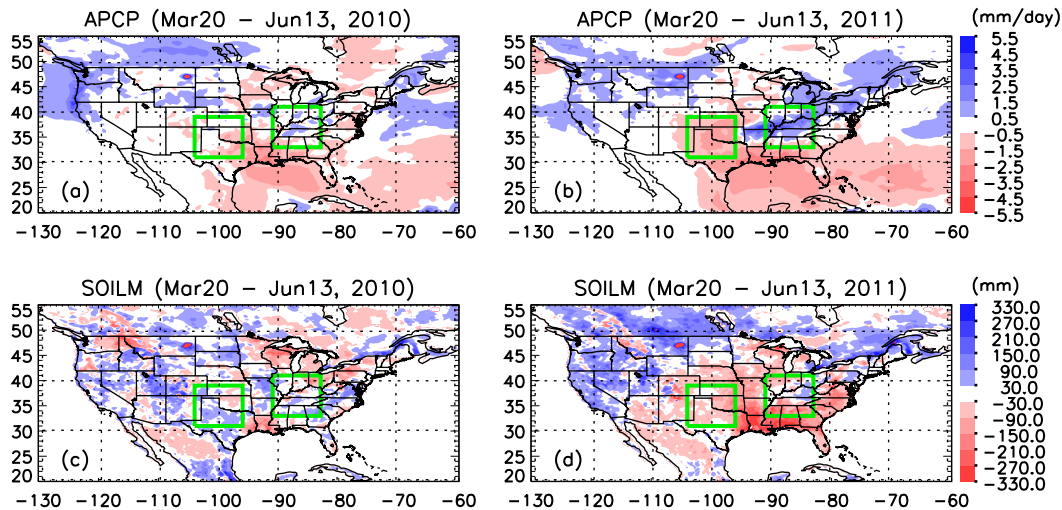


FIG. 1. Anomaly in (a) precipitation and (c) soil moisture from 20 Mar to 13 Jun 2010 with respect to the base period 1979–2013. (b), (d) As in (a), (c), but for 2011.

tropics and were mainly responsible for the hot and dry conditions in the southwestern United States (Wang et al. 2014). The spring of 2011 was particularly interesting because many rainfall and drought extremes occurred in the United States during this period. The lower Mississippi River experienced one of the worst floods in recent history, caused by extreme rainfall in the Ohio Valley in late April and early May. In the following, we will show the general meteorological conditions in the springs of 2010 and 2011 as compared with climatology (based on the period 1979–2013) using the NARR data.

Even though the La Niña condition was not formally established until June, the precipitation anomaly from 20 March to 13 June 2010 resembles a weak La Niña condition, with positive anomalies in the northwest and negative anomalies in the southeast (Fig. 1a). During 2011, the negative anomalies extended farther westward to Texas and Arkansas (Fig. 1b), showing a much stronger influence of the La Niña condition. The soil moisture indicates a very dry year in the southern and southeastern United States in 2011 (Fig. 1d), with only a small area of positive anomalies in the center of the Ohio Valley, which is likely due to the heavy precipitation in this area during late April and early May (Fig. 2b). The soil moisture anomaly in 2010 is mostly positive over the entire CONUS, except over the Great Lakes and the Northeast. Based on precipitation and soil moisture anomalies in Texas and the lower midwestern regions in these two years, we broadly categorize 2011 as a dry year and 2010 as a relatively wet year.

For the purpose of comparison, we select two regions—one in the Midwest in northern Texas and Oklahoma and the other in the central Mississippi valley

(boxes in Fig. 1)—to represent the dry and wet regions, respectively. These two regions are very sensitive to the location and strength of Pacific jet stream and moisture inflow from the Gulf of Mexico (Higgins et al. 1997; Weaver et al. 2002). For the dry region, three relatively large episodes of precipitation events can be seen around 14 April, 15 May, and 14 June 2010, boosting up the otherwise low precipitation in the region (Fig. 2a). Soil moisture is slightly above the climatology before June and decreases to slightly below climatology after June (Fig. 2c). In the wet region, precipitation is close to the climatology for most of the period in 2010, with slightly above normal precipitation during the transition period from mid-April to early May (Fig. 2b). The soil moisture is also very close to the climatology in the region (Fig. 2d). In 2011, the precipitation is consistently below the climatology in the dry region because of a lack of any significant rain events (Fig. 2a). The soil moisture is much drier than the climatology for the entire period (Fig. 2c). In the wet region, even though soil moisture is much below the climatology (Fig. 2d), the precipitation is not significantly below the climatology (Fig. 2b). On the contrary, during the period from 15 April to 5 May 2011, there are many episodes of heavy precipitation events in the Midwest and the Ohio Valley, which led to the worst flood in recorded history in the lower Mississippi River. The excessive rainfall over the northern states (e.g., over the Ohio Valley) and severe drought in Texas and New Mexico in 2011 are consistent with a typical La Niña condition due to northward shift of the Pacific jet stream (Ting and Wang 1997; Kumar and Hoerling 1998).

The soil moisture in the two regions has a clear impact on the surface flux exchange and atmospheric boundary

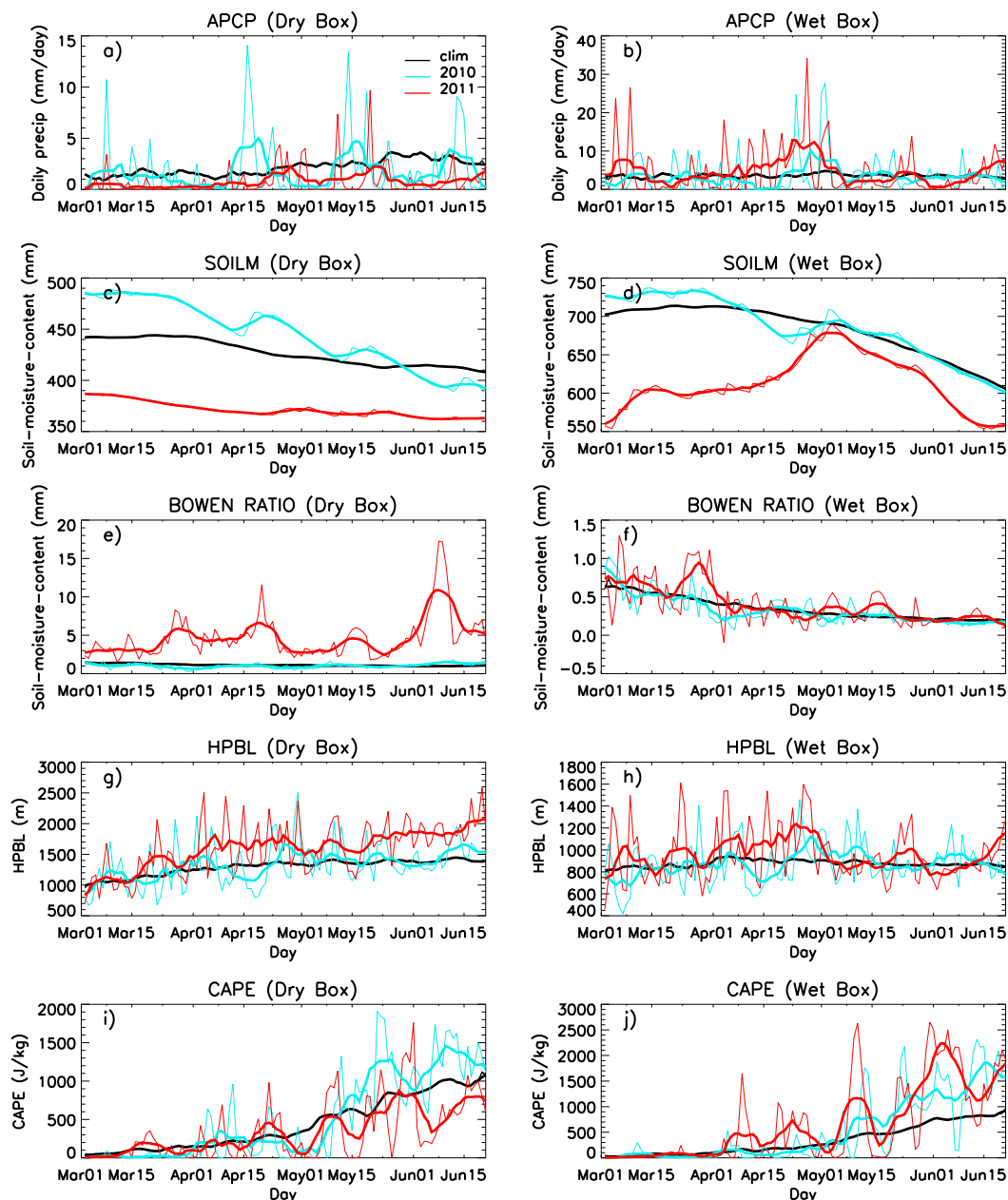


FIG. 2. Domain-averaged precipitation, soil moisture, Bowen ratio, HPBL, and CAPE during 1 Mar and 15 Jun 2010 (cyan lines), 1 Mar and 15 Jun 2011 (red lines), and climatology (black lines, computed from the period 1979–2013) in (left) dry and (right) wet regions, respectively. Thin and thick lines are daily and 5-day running means, respectively.

conditions. In the dry region, higher Bowen ratio and planetary boundary layer height (PBLH) are observed, which is consistent with much drier soil moisture in the spring of 2011 than in 2010 (Figs. 2e,g). Whether the dry soil moisture had further suppressed precipitation in the dry region in 2011 is a question to be answered (Betts and Ball 1998; Eltahir 1998). In the wet region, even though the soil moisture in 2011 is much below its climatology in

the region, it is higher than that in the dry region (Fig. 2d). The Bowen ratio in the wet region is much smaller than the dry region and remains close to climatology even though the soil moisture in 2011 is much lower (Fig. 2f). The small variability in Bowen ratio could limit the impact of soil moisture on precipitation in the wet region. Convective available potential energy (CAPE) is low in the early spring in both regions and increases quickly starting

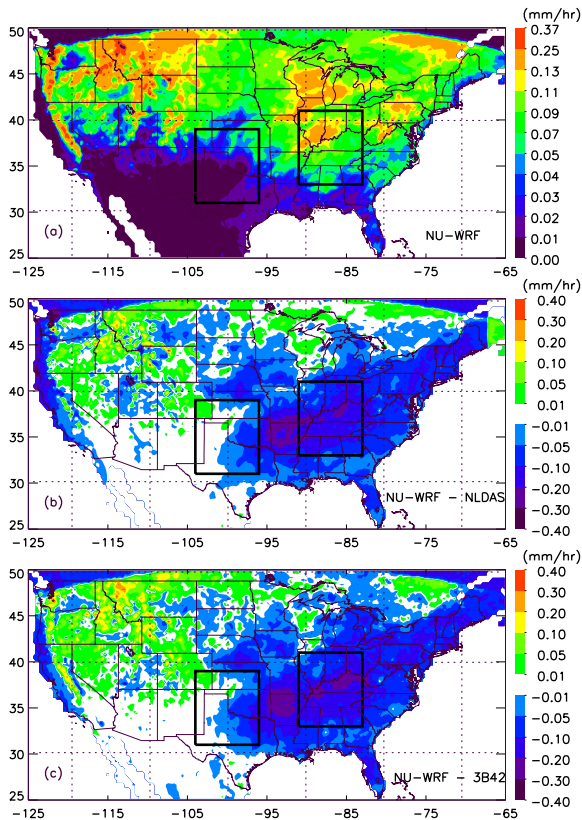


FIG. 3. (a) NU-WRF simulated mean precipitation intensity from 20 Mar to 13 Jul 2011. (b) Difference between NU-WRF and NLDAS. (c) Difference between NU-WRF and 3B42.

in late April (Figs. 2i,j). In the dry region, CAPE is higher in 2010 than in 2011, while in the wet region, it is higher in 2011, consistent with the observed precipitation in these two regions.

In the following, we will show the NU-WRF simulations of precipitation in these two seasons. The questions we want to answer are 1) if and how precipitation responds to the change of soil moisture in 2010 and 2011; 2) if the relationship of the two is location dependent, such as in the dry and wet regions; 3) how important the large-scale circulation and moisture convergence is as compared with local soil moisture and localized surface evaporation; and 4) is there scale dependence of land-atmosphere interaction as revealed by the moisture budget of precipitation?

b. Model simulations of heavy and light rain

Before discussing the sensitivity tests, we will briefly compare NU-WRF simulations with observations to assess the model's capability and limitation in simulating individual precipitation events as well as total precipitation in the 3-month period. Figure 3 shows the accumulated precipitation from the model's

original run (driven by large-scale forcing and soil moisture of the same year; S11-org in Table 1) and the biases with respect to the two observational datasets for the period from 20 March to 13 June 2011. The NU-WRF has roughly captured the spatial distribution of rainfall within the CONUS, with heavy precipitation in the Northwest and central Northeast and less precipitation in the Southwest. The model tends to overestimate precipitation in the northern and northwestern regions but underestimate it in the central and southeastern United States, a feature quite common in regional climate model (RCM) simulations (Mearns et al. 2012). The bias maps from the two observational datasets are quite similar, which increases the confidence in the observed precipitation. The large negative bias along the Mississippi and Ohio Valley indicates significant underestimates of heavy precipitation in these areas, which might result from the model's poor simulation of upper- and lower-level jets critical to the moisture convergence in the region (Higgins et al. 1997; Mo and Berbery 2004). Previous studies indicate that spatial nudging could improve the results by improving the large-scale forcing further into the domain center (Miguez-Macho et al. 2005). However, nudging will interrupt the physical processes of a free run by pushing the forecasted states (e.g., temperature, moisture, and wind) to be closer to the forcing datasets (i.e., NARR) whether land-atmosphere interaction is working or not, thus defying the purpose of this study, which aims to understand the mechanism and feedback of the land-atmosphere interaction. The possible impact of this model bias in the simulation of heavy precipitation events will be included in the discussion of results.

The domain-averaged time series for the wet and dry regions show that the model captures the main episodes of precipitation and timing long after its initialization time in April and May, but underestimates the intensity of heavy rain (Fig. 4). The forecast skill declines with longer forecast time and the model misses more precipitation episodes entering the second half of June, so the analysis is cut off on 13 June. The mean precipitation intensity from NU-WRF for the period from 20 March to 13 June is about 54% and 43% of that from NLDAS for the dry and wet regions. While these results are not ideal for quantitative seasonal forecasts, they are comparable with similar studies (Mearns et al. 2012; Bukovsky et al. 2013). Many previous studies have shown that model configurations, for example, domain size, spatial resolution, nudging, as well as large-scale forcing and physical parameterizations, could affect the simulations (Done et al. 2005; Miguez-Macho et al. 2005);

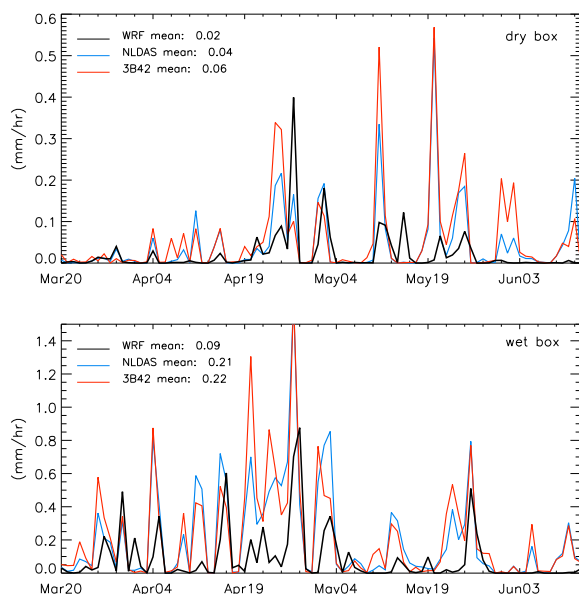


FIG. 4. Domain mean daily precipitation from 20 Mar to 13 Jun 2011 in (top) dry and (bottom) wet box.

however, it is not the focus of this study to achieve the best model simulations. The impact of model configuration and physical scheme in short-term simulations will be a discussed in a separate paper.

c. Impact of large-scale forcing and soil moisture to precipitation

To understand the effect of soil moisture and large-scale forcing on precipitation, we swapped the soil moisture in 2010 and 2011 to produce four simulations (Table 1). The domain-averaged moisture budgets for the entire period are listed in Tables 2 and 3 for the dry and wet regions, respectively. In the dry region, the large-scale forcing creates a larger difference in moisture convergence ($S11\text{-swp} - S10\text{-org}$) while the soil moisture creates a larger difference in evaporation ($S10\text{-swp} - S10\text{-org}$) (Table 4). The precipitation difference from the years 2011 and 2010 (-0.011 mm h^{-1} ; $S11\text{-org} - S10\text{-org}$) is more likely due to differing large-scale forcing (-0.008 mm h^{-1} ; $S11\text{-swp} - S10\text{-org}$) than differing soil moisture (-0.005 mm h^{-1} ; $S10\text{-swp} - S10\text{-org}$) (Table 4). In essence, substituting the

2010 soil moisture with the drier soil moisture of 2011 would create a 21% reduction of mean precipitation in 2010. Likewise, mean precipitation would increase by 23% in 2011 if the wetter soil moisture of 2010 were used. In the wet region, both large-scale forcing and soil moisture have a relatively small effect on precipitation (Table 5).

The large difference of precipitation in the dry region can be further explained using Fig. 5. In the S11-org simulation, dry soil moisture prevails in the southern United States, especially in the Southwest as compared to the S11-swp simulation (Fig. 5b). This leads to higher sensible heat flux (SH; Fig. 5c) and lower latent heat flux (LH; Fig. 5d) that contributes to higher Bowen ratio (Fig. 5g) and PBLH (Fig. 5f) in the Southwest, as predicted by Betts and Ball (1998). The elevated Bowen ratio and PBLH can be observed in the dry year simulations in the entire period (Fig. 6), especially before precipitation events, as shown in Fig. 6a. High PBLH is a result of the dry boundary, low equivalent potential temperature, and likely more entrainment of dry, free atmosphere in the planetary boundary top (Betts et al. 1996), suppressing convection as a result. On the other hand, the net increase in surface radiation is contrary to reduced net surface radiation from increased albedo, as suggested in Eltahir (1998) (Fig. 5e). One reason could be that the standard Noah LSM used by LIS has not included a dynamic albedo scheme that changes with soil moisture (Zaitchik et al. 2013). More importantly, a net increase in surface radiation is mainly due to reduced cloud and precipitation under the dry conditions. Also, lower moisture convergence is simulated in S11-org than in S11-swp in the dry region, indicating that a feedback from surface moisture to large-scale circulations has occurred (Fig. 5h).

The relative importance of large-scale forcing and soil moisture is further illustrated in Fig. 7. In Figs. 7a and 7b, the difference in geopotential height and wind in 850 and 200 mb from two large-scale forcing simulations with the same soil moisture (2011; $S11\text{-org} - S10\text{-swp}$) are shown. The figure shows that low pressure anomalies in 2011 cover almost the entire CONUS in 850 mb, with the exception of the Southwest and Northeast. This low system deepens in 200 mb, where a deep trough extends into the Gulf of Mexico, with a

TABLE 2. Dry region moisture budget in the atmosphere from four simulations (mm h^{-1}). EVAP, MCONV, and PREC refer to surface evaporation, vertically integrated moisture convergence, and precipitation, respectively.

Simulation	Mean EVAP	Mean MCONV	Mean PREC	Change in storage
S10-org	0.066	-0.035	0.024	0.007
S10-swp	0.050	-0.029	0.019	0.002
S11-org	0.043	-0.046	0.013	-0.015
S11-swp	0.059	-0.059	0.016	-0.015

TABLE 3. As in Table 2, but for wet region.

Simulation	Mean EVAP	Mean MCONV	Mean PREC	Change in storage
S10-org	0.170	−0.004	0.096	0.070
S10-swp	0.173	−0.027	0.095	0.051
S11-org	0.160	−0.013	0.101	0.046
S11-swp	0.155	0.001	0.096	0.060

high pressure center located in the Midwest. This circulation pattern directly contributes to dry conditions in the Southwest and facilitates more moisture being transferred from the Gulf of Mexico, causing heavy precipitation along the upper Ohio Valley. Figures 7c and 7d show the circulation difference using the same large-scale forcing (2011) but different soil moisture (S11-org − S11-swp). They show that using the dry soil moisture of 2011 as compared to the relatively wet soil moisture of 2010 would induce a positive anomaly in geopotential height in the Southeast and Northwest and a negative anomaly in the Southwest and Northeast. In the upper atmosphere, the entire CONUS was under positive geopotential height anomaly, except in the Northwest. This illustrates that the feedback due to soil moisture can affect the circulation, but the impact of soil moisture on circulation is an order of magnitude smaller than the difference introduced by different large-scale forcings.

d. Scale dependence

There are many pathways that soil moisture can affect precipitation through evapotranspiration, radiation, and boundary layer processes. In the above section, we have shown that soil moisture could affect surface heat flux, planetary boundary layer, and feedback into large-scale circulations. Ultimately, all these effects can be traced back to precipitation moisture sources: evaporation, moisture convergence, and moisture storage in the atmosphere. Assuming the liquid and ice water amounts from cloud advection are negligible, the moisture budget equation takes the form (Rasmusson 1968, 1971; Yanai et al. 1973)

$$\langle P - E \rangle = \left\langle \frac{1}{g} \int_s^t \nabla \cdot V q dp \right\rangle + \left\langle \frac{\partial}{\partial t} \frac{1}{g} \int_s^t q dp \right\rangle. \quad (1)$$

Here, P , E , V , q , g , and p are precipitation, evaporation, wind, specific humidity, acceleration of gravity, and

pressure, respectively; angle brackets represent time average; s and t refer to the lower (surface) and upper (tropopause) bounds, respectively, for the vertical integration $1/g \int_s^t dp$.

The first term on the right-hand side accounts for the horizontal moisture convergence (MCONV), and the second term represents a change of column water vapor in the atmosphere. By tracking the changes in surface evaporation and moisture convergence, we can quantify the net effect of soil moisture on precipitation. However, since precipitation is highly nonlinear and intermittent in nature, being largely controlled by synoptic-scale forcing, the effect of soil moisture on precipitation will vary significantly for individual precipitation events, as well as for the temporal and spatial scales in question (Zangvil et al. 2001). It has been suggested that such moisture budget analysis requires a minimum size from 0.6×10^6 to $1.0 \times 10^6 \text{ km}^2$ (Rasmusson 1968, 1971; Yanai et al. 1973). This is approximately the size of the domain in this study. In the following, we will illustrate the effects of soil moisture as a function of spatial and temporal scales using a moisture budget analysis method. We hope to provide a qualitative as well as a quantitative estimate of soil moisture effect under different situations.

1) MOISTURE BUDGETS OF SINGLE RAIN EVENTS

It is well known that water cycles through surface and atmosphere, land and ocean, tropics and polar regions. Over a long period (a year or more), the total precipitation will be roughly balanced by total evaporation and ground runoff. From the viewpoint of a single precipitation event, both the atmospheric thermodynamic conditions (boundary instability and CAPE) and moisture supply (prestored as soil moisture and precipitable water in the atmosphere) are a result of accumulated meteorological conditions long before the actual event (Trenberth et al. 2003). The

TABLE 4. Moisture budget differences between the simulations for the dry region (mm h^{-1}).

Comparison cases	Δ Mean EVAP	Δ Mean MCONV	Δ Mean PREC	Δ Change in storage
S11-org − S10-org	−0.023	−0.011	−0.011	0.0
Soil moisture effect: S10-swp − S10-org	−0.016	0.006	−0.005	−0.005
Large-scale forcing effect: S11-swp − S10-org	−0.007	−0.021	−0.008	−0.022

TABLE 5. As in Table 4, but for wet region.

Comparison cases	$\Delta\text{Mean EVAP}$	$\Delta\text{Mean MCONV}$	$\Delta\text{Mean PREC}$	$\Delta\text{Change in storage}$
S11-org – S10-org	–0.010	–0.009	0.005	–0.024
Soil moisture effect: S10-swp – S10-org	0.003	–0.023	–0.001	–0.019
Large-scale forcing effect: S11-swp – S10-org	–0.015	0.005	0.0	–0.010

prestorm moisture storages are determined by continuous moisture convergence and surface evaporation before the storm. Therefore, to account for the moisture budget of a precipitation event, it is necessary to define the window of events.

Assuming a precipitation event ends at day 0, if we consider the moisture contribution to the event starts from d (days) before (designated as $-d$) regardless of its actual starting time, the moisture budget for this particular event is thus an integration from $-d$ to 0 (Fig. 8):

$$AV_{-d} = AV_{-d \rightarrow 0} = \sum_{t=-d}^0 V_t. \quad (2)$$

This is equivalent to considering the precipitation event in a window size of d (days). Here, A represents an accumulation over the time period. The parameter V represents parameters of interest, such as precipitation (PREC), moisture convergence, and evaporation (EVAP), so that APREC, AEVAP, and AMCONV represent accumulated precipitation, evaporation, and moisture convergence, respectively. The moisture budget terms and their relative contributions are obviously a function of the window size d . The smaller d value (closer to the right end of the x axis) indicates a smaller window of consideration before the rain event.

Figure 8 shows the integrated moisture budget leading to the heaviest rain event as a function of the leading time during the simulation period in 2010 in the wet and dry regions, respectively. Note that the moisture fluxes in this figure are accumulated backward starting from the rightmost point (end of major rain event). In the wet region, there are several lighter rain events that occurred during the 40-day period before the heaviest rain event (Fig. 8a). This figure shows that if we consider the rain event as a 40-day process, total evaporation (black lines) accumulated during this period is larger than the total moisture convergence (light blue lines) during this period. The total evaporation decreases steadily as the window size decreases. The total moisture convergence, however, is not a monotonic increasing or decreasing curve with the window size, as moisture

can converge or diverge out of the region during a given period, which is controlled by large-scale forcing. It is likely to increase before a major rain event and then decrease after the rain event. Close to the precipitation event (1–2 days lead time), the moisture convergence is found to be much larger than the evaporation. For a medium-sized window (up to 12 days), it can be seen that the combined evaporation and moisture convergence roughly balances the precipitation. For a lead time that is longer than 12 days, precipitation is slightly less than the summation of evaporation and moisture convergence. A small deposit could be within precipitating clouds that have not yet rained out, but mostly because the atmosphere can hold more precipitable water as temperatures warm up during the late spring and early summer.

In the dry region, we notice a very different scenario. Before the rain event on 16 May 2010, there are a few light precipitation events (Fig. 8b). Evaporation and moisture convergence nearly cancel each other for the longer period, as evaporation basically provides the moisture source to be divergent out of the region. The moisture convergence could still be a major moisture source in the short term for a major rainfall event, when AMCONV is much larger than the AEVAP term on 3 to 1 days before the event. Inspecting other light events, we found that ACONV could be less than AEVAP even in near term (figures not shown). Without a sudden source of moisture convergence, precipitation occurs by depleting precipitable water stored in the atmosphere, with a relatively lower rain rate than the event on 16 May 2010.

Replacing the relatively wet soil moisture in 2010 (solid line) with dry soil moisture in 2011 (dashed line), we notice larger differences in both evaporation and moisture convergence in the dry region (Fig. 8b) than in the wet region (Fig. 8a). Dry soil moisture has resulted in less evaporation, and correspondingly, less moisture divergence. The effect on a single precipitation event is also noticeable, as there appears to be a small reduction of rain intensity on 16 May 2010.

2) DEPENDENCE OF MOISTURE BUDGET ON TEMPORAL SCALE

To examine the cumulative effect on total precipitation in the region, we integrate the three water budget terms

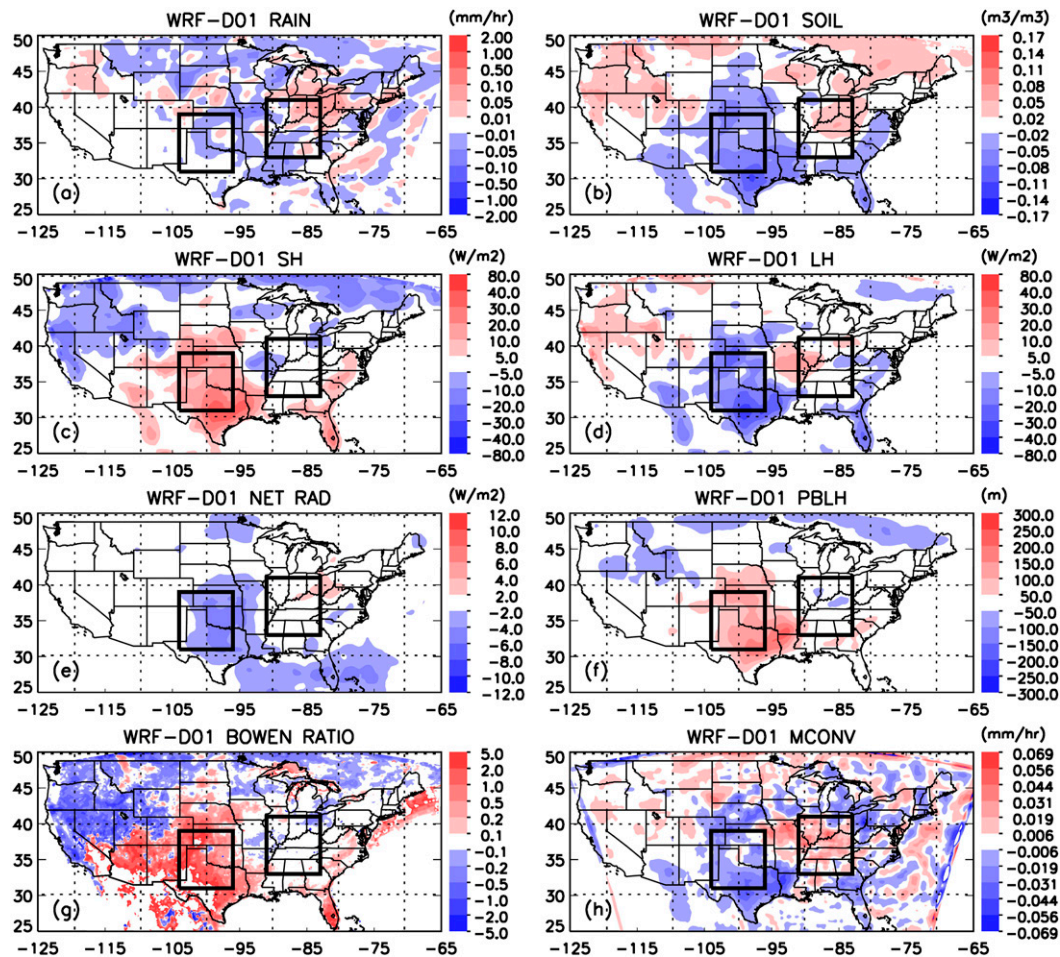


FIG. 5. Mean differences (S11-org – S11-swp) in rain rate and surface fluxes from 20 Mar to 13 Jun. The two simulations use large-scale forcing from 2011 and soil moisture from 2011 and 2010, respectively.

(precipitation, moisture convergence, and evaporation) from the beginning of the period to the end. The values in a given d in Figs. 9 and 10 are computed as

$$AV_{1 \rightarrow d} = \sum_{t=1}^d V_t. \quad (3)$$

For the wet region, we notice a steady increase of total moisture from evaporation as the integration days increase; the total moisture convergence increases slightly at the beginning but drops following the rain events (Fig. 9). There was a major jump around 30 April 2010 and 26 April 2011, slightly ahead of major rain events, and a decrease afterward into negative values by the end of the period. It is tempting to conclude that for periods longer than 60 days, local evaporation (and recycling water vapor) provides the major moisture supply for the total precipitation. However, the exact temporal scale required will depend on the season

and region of interest. Furthermore, even though evaporation provides the major moisture supply in the long period, the difference due to surface soil moisture is minimal to the total evaporation and precipitation in this case.

In the dry region, total evaporation steadily increases with time as well, albeit at only half the rate compared to the wet region (Fig. 10). The moisture convergence accumulates in a steady negative direction (which indicates divergence out of the region), with a small upward bump around 14 May 2010, which is also noticeable in total precipitation accumulation. The relatively large differences in evaporation and moisture convergence from the swapped soil moisture runs can be easily noticed. The dry soil moisture (dashed lines) leads to less evaporation, less divergence (due to lower precipitable water vapor and weaker moisture inflow along the south-central United States), and a net reduction in total precipitation (Tables 2 and 4). More importantly, these differences accumulate with time. This illustrates an important positive

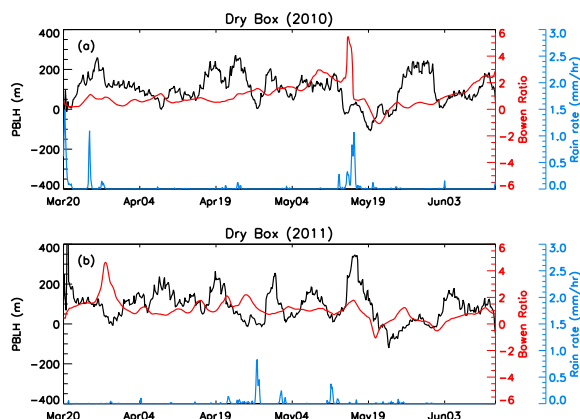


FIG. 6. (a) Domain mean differences ($S10\text{-swp} - S10\text{-org}$) in PBLH (black line) and Bowen ratio (red line) from 20 Mar to 13 Jun. Domain mean precipitation from $S10\text{-org}$ is shown by the blue line. (b) As in (a), but for the difference in simulations ($S11\text{-org} - S11\text{-swp}$). Domain mean precipitation from $S11\text{-org}$ is shown by the blue line. Note that in both years, the differences are computed from drier soil moisture simulation minus wetter soil moisture simulations.

feedback in the dry region, as previously reported (Shukla and Mintz 1982; Eltahir 1998).

3) DEPENDENCE OF MOISTURE BUDGET ON SPATIAL DOMAIN

The high spatial inhomogeneity of precipitation events prompts another necessity when considering the moisture budget, that is, selection of domain size and location. A domain chosen inside of a heavy rain event or a large domain encompassing surrounding areas is likely to come up with a different moisture budget. Here, we examine the relative contribution of moisture convergence and evaporation to precipitation as a function of domain size in wet and dry regions, respectively. The period considered is the entire simulation period, as the results for a short period could vary even more significantly with individual events and the center of the domain selected.

Figure 11a shows the domain mean total precipitation during the period from 20 March to 13 June in the dry region from all four simulations. The domain size increases from $0.25^\circ \times 0.25^\circ$ to $8^\circ \times 8^\circ$ grid boxes, with all of them centered on $(35^\circ\text{N}, 100^\circ\text{W})$. Note that the largest box of $8^\circ \times 8^\circ$ is about the size for the analysis in previous sections. The general increase of mean precipitation with domain size indicates that the center grid box is the driest spot in this area. Larger differences in precipitation are found between runs with different large-scale forcings (i.e., black vs red lines); smaller but distinctive differences are found between runs with different soil moisture (i.e., solid lines vs dashed lines). These results again show that the large-scale forcing dominates precipitation

distribution, but the impacts of soil moisture are obvious. In both years, using the drier soil moisture of 2011 has resulted in less precipitation, as indicated by the dashed lines in Fig. 11a, but the impact is not equal in the two years. The drier year 2011 (red lines in Fig. 11a) shows a smaller reduction of precipitation because of dry soil moisture. This is likely due to saturation effect, as mentioned in other studies (Seneviratne et al. 2006; Guo and Dirmeyer 2013; Lintner et al. 2013). When it is already very dry or wet, there is less room to be even drier or wetter.

To further examine the relationship of these moisture terms, we computed the ratio of evaporation to precipitation (E/P) and moisture convergence to precipitation (C/P) as a function of domain size for all the four simulations (Fig. 11b). The E/P ratio starts at around 4 for the $1^\circ \times 1^\circ$ box and asymptotes to about 2 for the $8^\circ \times 8^\circ$ box in 2011 (red lines with triangles). The E/P value starts with slightly less than 2 and remains quite stable at 2 for all domain sizes in 2010 (black lines with triangles). The C/P ratio has comparable magnitude but with a negative sign because of net moisture divergence in the dry region. Because of the large ratios of E/P and C/P and their opposite signs, the magnitude of precipitation is much smaller than the evaporation or convergence alone. It is natural to consider precipitation as a small residue of evaporation and convergence, with the drier year of 2011 more so than the relatively wet year of 2010. The E/P ratios from simulations with drier 2011 soil moisture ($S11\text{-org}$ and $S10\text{-swp}$) are slightly smaller than the simulations with wet soil moisture in the corresponding year ($S11\text{-swp}$ and $S10\text{-org}$, respectively). This increase in precipitation efficiency partially cancels out the positive feedback due to dry soil moisture (i.e., drier soil moisture \rightarrow less total evaporation \rightarrow less precipitation \rightarrow even drier soil moisture). The reduced magnitude of C/P could be simply due to less available moisture to be divergent out of the domain. However, it could also be due to circulation feedback as shown in Fig. 7. Obviously, the reduction is not able to completely cancel out the reduced evaporation. Hence, a net reduction in precipitation has occurred.

Spatially, there is a tendency for the simulations from different large-scale forcings to converge as the domain size increases. However, the difference due to different soil moisture tends to increase. The dry soil moisture tends to modulate the precipitation recycling efficiency in the dry region but was not enough to reverse the overall positive feedback in the dry region.

4. Summary and discussion

In this study, we conducted NU-WRF simulations of precipitation events during the spring and early

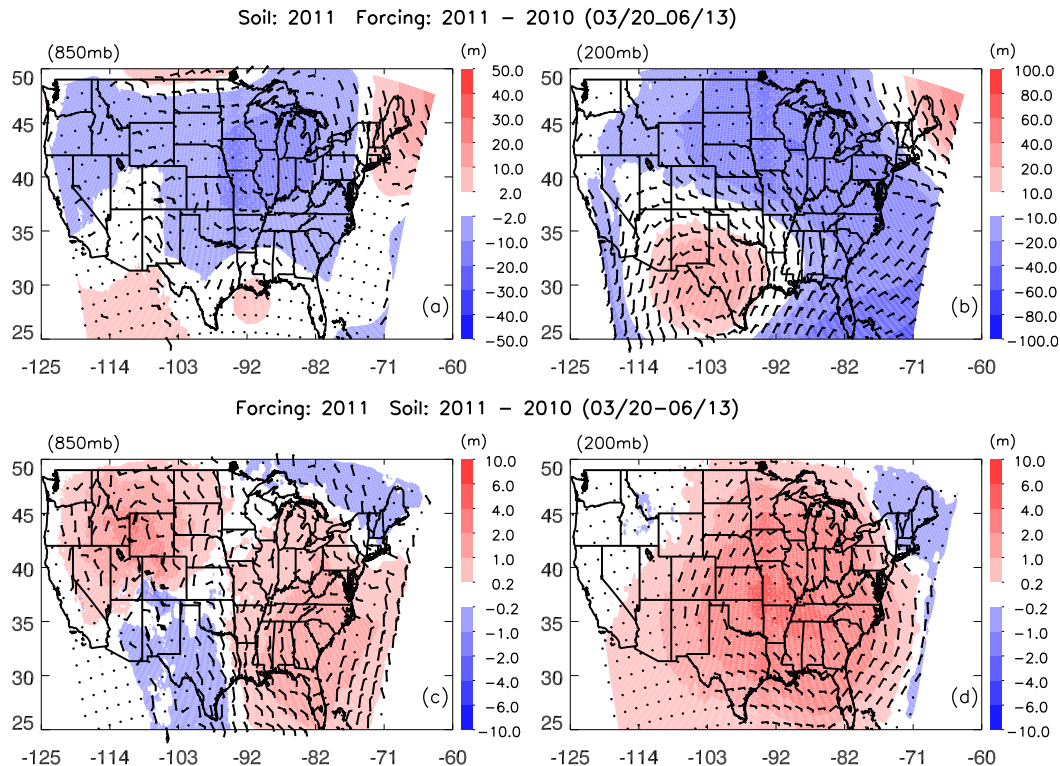


FIG. 7. Differences in geopotential height and wind from simulations ($S11\text{-org} - S10\text{-swp}$) in (a) 850 and (b) 200 mb. The two simulations use large-scale forcings from 2011 and 2010 but the same soil moisture from 2011. (c),(d) As in (a),(b), but for simulations ($S11\text{-org} - S11\text{-swp}$). The two simulations use the same large-scale forcing from 2011 but soil moisture from 2011 and 2010, respectively. Note that the color scales are an order of magnitude different in the top vs bottom.

summer of 2010 and 2011 in CONUS and examined the impacts of large-scale forcing and land-atmosphere interactions on precipitation in the dry and wet regions in the southwestern and south-central United States. Both springs are under fast transitions of ENSO phases: from El Niño to La Niña in 2010 and from La Niña to ENSO-neutral in 2011, which typically have large influences on precipitations in these two regions. Even though much extreme rainfall hit the Midwest and the Ohio Valley in late April and early May in 2011, based on soil moisture and total precipitation during the entire period, 2011 is drier than 2010 in both focus regions, showing a much stronger influence of La Niña conditions (Wang et al. 2014).

The NU-WRF simulations overestimate precipitation in the Northwest and underestimate it in the Southeast. They capture major precipitation episodes in the study domains but underestimate the mean and peak rain intensity. The simulated mean intensities for the period from 20 March to 13 June 2011 measure about 54% and 43% of the NLDAS observations in the dry and wet regions, respectively, possibly because of long integration,

lack of spatial nudging, and misrepresentation of upper- and lower-level jets.

Sensitivity studies of the springs of 2010 and 2011 with swapped soil moisture show that large-scale atmospheric forcing plays a major role in producing regional precipitation. Soil moisture has a larger impact in the dry region, where drier soil moisture in 2011 tends to further reduce the precipitation by approximately 23%, a positive feedback that could worsen the drought in Texas and lower midwestern regions, exacerbating La Niña conditions. It is found that drier soil moisture not only reduces total evaporation through prolonged periods over a large spatial domain, but it also leads to higher Bowen ratio and planetary boundary height, indicating a potential pathway of positive feedback in the dry region, as suggested by Betts et al. (1997) and similarly suggested by Brimelow et al. (2011a,b), in which they show soil moisture impacts convective activity through vegetation and boundary heights in the Canadian Prairies. The study also shows the asymmetric nature of soil moisture impact, with larger impacts found in the dry region and during the light rain events rather than the wet region

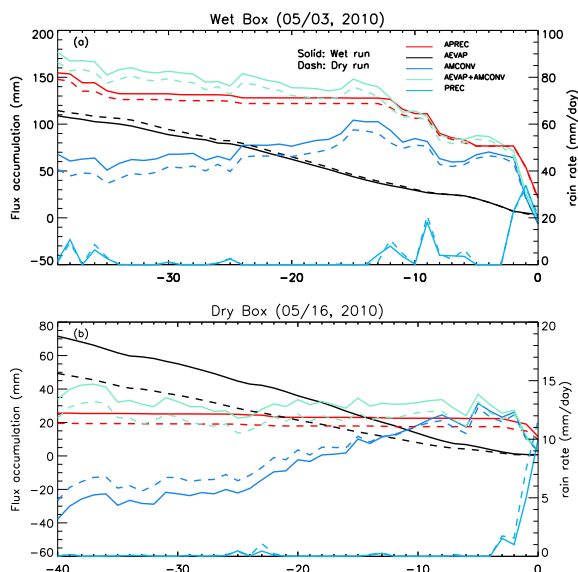


FIG. 8. (a) Moisture fluxes (APREC, AEVAP, AMCONV, and AEVAP + AMCONV) contributing to the precipitation event on 3 May 2010 (day 0) as a function of leading time in the wet region (scaled with left y axis) along with daily precipitation rate (PREC) (scaled in the right y axis). (b) As in (a), but for the event on 16 May 2010 in the dry region. Both events are heaviest in the respective region during the simulation period. The solid (dashed) lines are run with the wet (2010) and dry (2011) soil moisture, respectively.

and heavy rain events. This is consistent with findings from global modeling studies that show most significant coupling of soil moisture and precipitation occurs in transitional regions with modest rain amount and large variations of soil moisture (Koster et al. 2004; Schubert et al. 2008).

The sensitivity of precipitation to soil moisture can be analyzed with moisture budget in the atmosphere. We designed a methodology to account for moisture contributions to precipitation for individual precipitation events as well as total precipitation as a function of temporal and spatial scales under the same moisture budget framework. The analysis shows that the relative contributions of local evaporation and large-scale moisture convergence depend on the dry/wet regions and are a function of temporal and spatial scales. While the relative contributions vary with domain size and individual weather system, evaporation provides a major moisture source in the dry region and during light rain events, which leads to greater sensitivity to soil moisture in the dry region and during light rain events. The feedback of land surface processes to large-scale forcing is also noticed through changes in atmosphere circulation and moisture convergence.

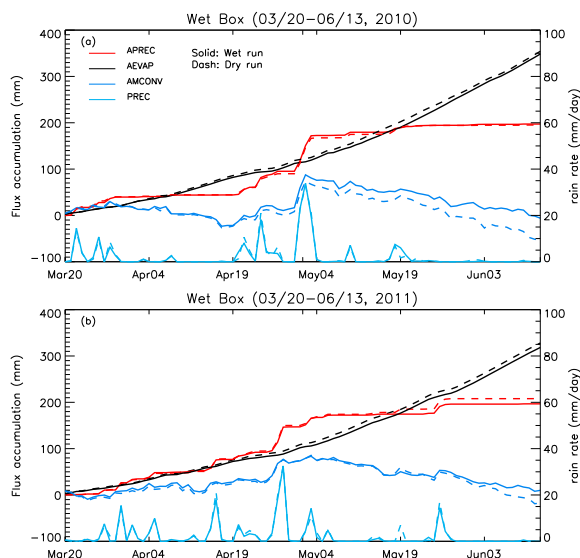


FIG. 9. Integrating precipitation (red), moisture convergence (blue), and evaporation (black) from 20 Mar to 13 Jun in the wet box in (a) 2010 and (b) 2011. The solid (dashed) lines are run with wet (2010) and dry (2011) soil moisture, respectively.

We should note that the results of this study depend on current model formulation and physics. As evident in the considerable dry model bias for heavy precipitation events, it is highly possible that the current model physics have not taken into account other important processes, such as the dynamics of the upper- and lower-level jets,

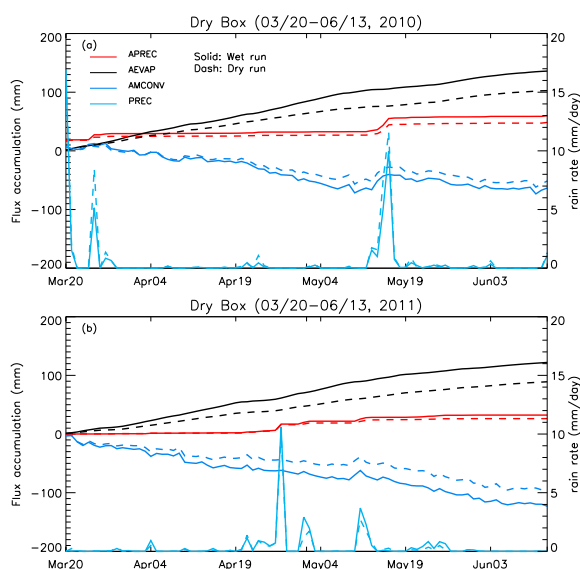


FIG. 10. Integrating precipitation (red), moisture convergence (blue), and evaporation (black) from 20 Mar to 13 Jun in the dry box in (a) 2010 and (b) 2011. The solid (dashed) lines are run with wet (2010) and dry (2011) soil moisture, respectively.

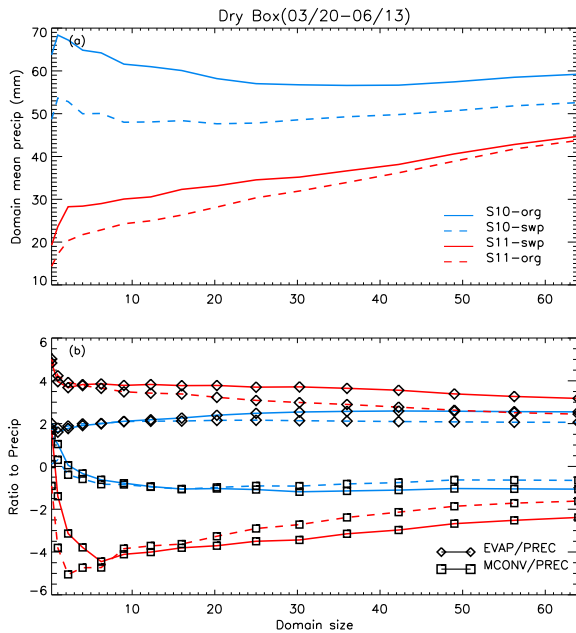


FIG. 11. (a) Mean precipitation as a function of domain size from four simulation runs. (b) Ratio of total evaporation and moisture convergence to total precipitation as a function of domain size. Red and black colors represent simulations with 2011 and 2010 large-scale forcing, and dashed and solid lines for runs with 2011 and 2010 soil moisture. Diamonds and squares represent ratio of evaporation and moisture convergence to precipitation, respectively. The domain size is in unit of square degree and centered in (35°N, 100°W).

the albedo dependence on soil moisture. (Hong and Pan 1998; Barros and Hwu 2002; Betts 2009; Seneviratne et al. 2013; Nicholson 2015). The lack of response to soil moisture in the wet region may be related to the problem of the model underestimating the magnitude of heavy rain. Hence, results shown in this work on soil moisture feedback can only be considered tentative and need to be validated with more case studies and model intercomparison studies.

Acknowledgments. This work was supported by NASA Precipitation Measuring Mission under Project NNX13AF73G. Computational and storage support was provided by NASA's Center for Climate Simulation (NCCS). We also thank two anonymous reviewers for their helpful comments.

REFERENCES

Barnston, A. G., M. H. Glantz, and Y. He, 1999: Predictive skill of statistical and dynamical climate models in SST forecasts during the 1997–98 El Niño episode and the 1998 La Niña onset. *Bull. Amer. Meteor. Soc.*, **80**, 217–243, doi:10.1175/1520-0477(1999)080<0217:PSOSAD>2.0.CO;2.

Barros, A. P., and W. Hwu, 2002: A study of land–atmosphere interactions during summertime rainfall using a mesoscale model. *J. Geophys. Res.*, **107**, 4227, doi:10.1029/2000JD000254.

Beljaars, A. C. M., P. Viterbo, M. J. Miller, and A. K. Betts, 1996: The anomalous rainfall over the United States during July 1993: Sensitivity to land surface parameterization. *Mon. Wea. Rev.*, **124**, 362–383, doi:10.1175/1520-0493(1996)124<0362:TAROTU>2.0.CO;2.

Betts, A. K., 2009: Land-surface–atmosphere coupling in observations and models. *J. Adv. Model. Earth Syst.*, **1**, doi:10.3894/JAMES.2009.1.4.

—, and J. H. Ball, 1998: FIFE surface climate and site-average dataset 1987–89. *J. Atmos. Sci.*, **55**, 1091–1108, doi:10.1175/1520-0469(1998)055<1091:FSCASA>2.0.CO;2.

—, —, A. C. M. Beljaars, M. J. Miller, and P. Viterbo, 1996: The land surface–atmosphere interaction: A review based on observational and global modeling perspectives. *J. Geophys. Res.*, **101**, 7209–7225, doi:10.1029/95JD02135.

Betts, R. A., P. M. Cox, S. E. Lee, and F. I. Woodward, 1997: Contrasting physiological and structural vegetation feedbacks in climate change simulations. *Nature*, **387**, 796–799, doi:10.1038/42924.

Bosilovich, M. G., and S. D. Schubert, 2002: Water vapor tracers as diagnostics of the regional hydrologic cycle. *J. Hydrometeor.*, **3**, 149–165, doi:10.1175/1525-7541(2002)003<0149:WVTADO>2.0.CO;2.

—, and J. Chern, 2006: Simulation of water sources and precipitation recycling for the MacKenzie, Mississippi, and Amazon River basins. *J. Hydrometeor.*, **7**, 312–329, doi:10.1175/JHM501.1.

Brimelow, J. C., J. M. Hanesiak, and W. R. Burrows, 2011a: Impacts of land–atmosphere feedbacks on deep, moist convection on the Canadian Prairies. *Earth Interact.*, **15**, doi:10.1175/2011E1407.1.

—, —, and —, 2011b: On the surface–convection feedback during drought periods on the Canadian Prairies. *Earth Interact.*, **15**, doi:10.1175/2010E1381.1.

Brubaker, K. L., D. Entekhabi, and P. S. Eagleson, 1993: Estimation of continental precipitation recycling. *J. Climate*, **6**, 1077–1089, doi:10.1175/1520-0442(1993)006<1077:EOCPR>2.0.CO;2.

—, P. A. Dirmeyer, A. Sudjarat, B. S. Levy, and F. Bernal, 2001: A 36-yr climatological description of the evaporative sources of warm-season precipitation in the Mississippi River basin. *J. Hydrometeor.*, **2**, 537–557, doi:10.1175/1525-7541(2001)002<0537:AYCDOT>2.0.CO;2.

Budyko, M. I., 1974: *Climate and Life*. Academic Press, 508 pp.

Bukovsky, M. S., D. J. Gochis, and L. O. Mearns, 2013: Towards assessing NARCCAP regional climate model credibility for the North American monsoon: Current climate simulations. *J. Climate*, **26**, 8802–8826, doi:10.1175/JCLI-D-12-00538.1.

Charney, J. G., W. J. Quirk, S.-H. Chow, and J. Kornfield, 1977: Comparative study of effects of albedo change on drought in semiarid regions. *J. Atmos. Sci.*, **34**, 1366–1385, doi:10.1175/1520-0469(1977)034<1366:ACSOTE>2.0.CO;2.

Chin, M., R. B. Rood, S.-J. Lin, J. F. Muller, and A. M. Thompson, 2000: Atmospheric sulfur cycle in the global model GOCART: Model description and global properties. *J. Geophys. Res.*, **105**, 24 671–24 687, doi:10.1029/2000JD900384.

Chou, M.-D., and M. J. Suarez, 1999: A shortwave radiation parameterization for atmospheric studies. NASA/TM-1999-104606, Vol. 15, 38 pp. [Available online at <http://gmao.gsfc.nasa.gov/pubs/docs/Chou136.pdf>.]

Conil, S., H. Douville, and S. Tyteca, 2007: The relative influence of soil moisture and SST in climate predictability explored within

- ensembles of AMIP type experiments. *Climate Dyn.*, **28**, 125–145, doi:[10.1007/s00382-006-0172-2](https://doi.org/10.1007/s00382-006-0172-2).
- Cook, B. I., G. B. Bonan, and S. Levis, 2006: Soil moisture feedbacks to precipitation in South Africa. *J. Climate*, **19**, 4198–4206, doi:[10.1175/JCLI3856.1](https://doi.org/10.1175/JCLI3856.1).
- Dirmeyer, P. A., and K. L. Brubaker, 1999: Contrasting evaporative moisture sources during the drought of 1988 and the flood of 1993. *J. Geophys. Res.*, **104**, 19 383–19 397, doi:[10.1029/1999JD900222](https://doi.org/10.1029/1999JD900222).
- , R. D. Koster, and Z. Guo, 2006: Do global models properly represent the feedback between land and atmosphere? *J. Hydrometeorol.*, **7**, 1177–1198, doi:[10.1175/JHM532.1](https://doi.org/10.1175/JHM532.1).
- Done, J. M., L. R. Leung, C. A. Davis, and Y. H. Kuo, 2005: Simulation of warm season rainfall using WRF Regional Climate Model. *6th WRF/15th MM5 Users' Workshop*, Boulder, CO, University Corporation for Atmospheric Research, 9.2. [Available online at <http://n2t.net/ark:/85065/d7gb2355>.]
- Douville, H., 2002: Influence of soil moisture on the Asian and African monsoons. Part II: interannual variability. *J. Climate*, **15**, 701–720, doi:[10.1175/1520-0442\(2002\)015<0701:IOSMOT>2.0.CO;2](https://doi.org/10.1175/1520-0442(2002)015<0701:IOSMOT>2.0.CO;2).
- Ek, M. B., K. E. Mitchell, Y. Lin, E. Rogers, P. Grunmann, V. Koren, G. Gayno, and J. D. Tarpley, 2003: Implementation of Noah land surface model advances in the National Centers for Environmental Prediction operational mesoscale Eta model. *J. Geophys. Res.*, **108**, 8851, doi:[10.1029/2002JD003296](https://doi.org/10.1029/2002JD003296).
- Eltahir, E. A. B., 1998: A soil moisture rainfall feedback mechanism: 1. Theory and observations. *Water Resour. Res.*, **34**, 765–776, doi:[10.1029/97WR03499](https://doi.org/10.1029/97WR03499).
- , and R. L. Bras, 1994: Precipitation recycling in the Amazon basin. *Quart. J. Roy. Meteor. Soc.*, **120**, 861–880, doi:[10.1002/qj.49712051806](https://doi.org/10.1002/qj.49712051806).
- Grell, G. A., and D. Devenyi, 2002: A generalized approach to parameterizing convection combining ensemble and data assimilation techniques. *Geophys. Res. Lett.*, **29**, 1693, doi:[10.1029/2002GL015311](https://doi.org/10.1029/2002GL015311).
- Guo, Z., and P. A. Dirmeyer, 2013: Interannual variability of land-atmosphere coupling strength. *J. Hydrometeorol.*, **14**, 1636–1646, doi:[10.1175/JHM-D-12-0171.1](https://doi.org/10.1175/JHM-D-12-0171.1).
- Higgins, R. W., Y. Yao, E. S. Yarosh, J. E. Janowiak, and K. C. Mo, 1997: Influence of the Great Plains low-level jet on summertime precipitation and moisture transport over the central United States. *J. Climate*, **10**, 481–507, doi:[10.1175/1520-0442\(1997\)010<0481:IOTGPL>2.0.CO;2](https://doi.org/10.1175/1520-0442(1997)010<0481:IOTGPL>2.0.CO;2).
- , W. Shi, E. Yarosh, and R. Joyce, 2000: Improved United States precipitation quality control system and analysis. NCEP/Climate Prediction Center Atlas 7. [Available online at http://www.cpc.ncep.noaa.gov/products/outreach/research_papers/ncep_cpc_atlas/7/.]
- , Y. Zhou, and H.-K. Kim, 2001: Relationships between El Niño–Southern Oscillation and the Arctic Oscillation: A climate–weather link. NCEP/Climate Prediction Center Atlas 8. [Available online at http://www.cpc.ncep.noaa.gov/research_papers/ncep_cpc_atlas/8/toc.html.]
- Hong, S.-Y., and H.-L. Pan, 1998: Convective trigger function for a mass-flux cumulus parameterization scheme. *Mon. Wea. Rev.*, **126**, 2599–2620, doi:[10.1175/1520-0493\(1998\)126<2599:CTFFAM>2.0.CO;2](https://doi.org/10.1175/1520-0493(1998)126<2599:CTFFAM>2.0.CO;2).
- Horel, J. D., and J. M. Wallace, 1981: Planetary-scale atmospheric phenomena associated with the Southern Oscillation. *Mon. Wea. Rev.*, **109**, 813–829, doi:[10.1175/1520-0493\(1981\)109<0813:PSAPAW>2.0.CO;2](https://doi.org/10.1175/1520-0493(1981)109<0813:PSAPAW>2.0.CO;2).
- Huffman, G. J., and Coauthors, 2007: The TRMM Multi-Satellite Precipitation Analysis (TMPA): Quasi-global, multiyear, combined sensor precipitation estimates at fine scales. *J. Hydrometeorol.*, **8**, 38–55, doi:[10.1175/JHM560.1](https://doi.org/10.1175/JHM560.1).
- Janjić, Z. I., 1994: The step-mountain Eta coordinate model: Further developments of the convection, viscous sublayer, and turbulence closure schemes. *Mon. Wea. Rev.*, **122**, 927–945, doi:[10.1175/1520-0493\(1994\)122<0927:TSMECM>2.0.CO;2](https://doi.org/10.1175/1520-0493(1994)122<0927:TSMECM>2.0.CO;2).
- Joussau, S., R. Sadourny, and J. Jouzel, 1984: A general-circulation model of water isotope cycles in the atmosphere. *Nature*, **311**, 24–29, doi:[10.1038/311024a0](https://doi.org/10.1038/311024a0).
- Kim, W., S.-W. Yeh, J.-H. Kim, J.-S. Kug, and M. Kwon, 2011: The unique 2009–2010 El Niño event: A fast phase transition of warm pool El Niño to La Niña. *Geophys. Res. Lett.*, **38**, L15809, doi:[10.1029/2011GL048521](https://doi.org/10.1029/2011GL048521).
- Koster, R., J. Jouzel, R. Suozzo, G. Russell, W. Broecker, D. Rind, and P. Eagleson, 1986: Global sources of local precipitation as determined by the NASA GISS GCM. *Geophys. Res. Lett.*, **13**, 121–124, doi:[10.1029/GL013i002p00121](https://doi.org/10.1029/GL013i002p00121).
- , and Coauthors, 2004: Regions of strong coupling between soil moisture and precipitation. *Science*, **305**, 1138–1140, doi:[10.1126/science.1100217](https://doi.org/10.1126/science.1100217).
- Kumar, A., and M. P. Hoerling, 1998: Annual cycle of Pacific–North American seasonal predictability associated with different phases of ENSO. *J. Climate*, **11**, 3295–3308, doi:[10.1175/1520-0442\(1998\)011<3295:ACOPNA>2.0.CO;2](https://doi.org/10.1175/1520-0442(1998)011<3295:ACOPNA>2.0.CO;2).
- Kumar, S. V., and Coauthors, 2006: Land information system: An interoperable framework for high resolution land surface modeling. *Environ. Modell. Software*, **21**, 1402–1415, doi:[10.1016/j.envsoft.2005.07.004](https://doi.org/10.1016/j.envsoft.2005.07.004).
- Lang, S., W.-K. Tao, R. Cifelli, W. Olson, J. Halverson, S. Rutledge, and J. Simpson, 2007: Improving simulations of convective system from TRMM LBA: Easterly and westerly regimes. *J. Atmos. Sci.*, **64**, 1141–1164, doi:[10.1175/JAS3879.1](https://doi.org/10.1175/JAS3879.1).
- , —, X. Zeng, and Y. Li, 2011: Reducing the biases in simulated radar reflectivities from a bulk microphysics scheme: Tropical convective systems. *J. Atmos. Sci.*, **68**, 2306–2320, doi:[10.1175/JAS-D-10-05000.1](https://doi.org/10.1175/JAS-D-10-05000.1).
- , —, J.-D. Chern, D. Wu, and X. Li, 2014: Benefits of a fourth ice class in the simulated radar reflectivities of convective systems using a bulk microphysics scheme. *J. Atmos. Sci.*, **71**, 3583–3612, doi:[10.1175/JAS-D-13-0330.1](https://doi.org/10.1175/JAS-D-13-0330.1).
- Lintner, B. R., P. Gentile, F. L. Findell, F. D'Andrea, A. H. Sobel, and G. D. Salvucci, 2013: An idealized prototype for large-scale land–atmosphere coupling. *J. Climate*, **26**, 2379–2389, doi:[10.1175/JCLI-D-11-00561.1](https://doi.org/10.1175/JCLI-D-11-00561.1).
- Matsui, T., and Coauthors, 2014: Introducing multi-sensor satellite radiance-based evaluation for regional earth system modeling. *J. Geophys. Res. Atmos.*, **119**, 8450–8475, doi:[10.1002/2013JD021424](https://doi.org/10.1002/2013JD021424).
- Mearns, L. O., and Coauthors, 2012: The North American Regional Climate Change Assessment Program: Overview of phase I results. *Bull. Amer. Meteor. Soc.*, **93**, 1337–1362, doi:[10.1175/BAMS-D-11-00223.1](https://doi.org/10.1175/BAMS-D-11-00223.1).
- Meehl, G. A., 1994: Influence of the land surface in the Asian summer monsoon: External conditions versus internal feedbacks. *J. Climate*, **7**, 1033–1049, doi:[10.1175/1520-0442\(1994\)007<1033:IOTLSI>2.0.CO;2](https://doi.org/10.1175/1520-0442(1994)007<1033:IOTLSI>2.0.CO;2).
- Meng, X. H., J. P. Evans, and M. F. McCabe, 2011: Numerical modelling and land-atmosphere feedback of drought in southeast Australia. *IAHS Publ.*, **344**, 144–149.
- Mesinger, F., and Coauthors, 2006: North American Regional Reanalysis. *Bull. Amer. Meteor. Soc.*, **87**, 343–360, doi:[10.1175/BAMS-87-3-343](https://doi.org/10.1175/BAMS-87-3-343).

- Miguez-Macho, G., G. L. Stenchikov, and A. Robock, 2005: Regional climate simulations over North America: Interaction of local processes with improved large-scale flow. *J. Climate*, **18**, 1227–1246, doi:[10.1175/JCLI3369.1](https://doi.org/10.1175/JCLI3369.1).
- Mitchell, K. E., and Coauthors, 2004: The multi-institution North American Land Data Assimilation System (NLDAS): Utilizing multiple GCIP products and partners in a continental distributed hydrological modeling system. *J. Geophys. Res.*, **109**, D07S90, doi:[10.1029/2003JD003823](https://doi.org/10.1029/2003JD003823).
- Mo, K. C., and E. H. Berbery, 2004: Low-level jets and the summer precipitation regimes over North America. *J. Geophys. Res.*, **109**, D06117, doi:[10.1029/2003JD004106](https://doi.org/10.1029/2003JD004106).
- Nicholson, S. E., 2015: Evolution and current state of our understanding of the role played in the climate system by land surface processes in semi-arid regions. *Global Planet. Change*, **133**, 201–222, doi:[10.1016/j.gloplacha.2015.08.010](https://doi.org/10.1016/j.gloplacha.2015.08.010).
- Notaro, M., Z. Liu, and J. W. Williams, 2006: Observed vegetation–climate feedbacks in the United States. *J. Climate*, **19**, 763–786, doi:[10.1175/JCLI3657.1](https://doi.org/10.1175/JCLI3657.1).
- Peters-Lidard, C. D., S. V. Kumar, D. M. Mocko, and Y. Tian, 2011: Estimating evapotranspiration with land data assimilation systems. *Hydrol. Processes*, **25**, 3979–3992, doi:[10.1002/hyp.8387](https://doi.org/10.1002/hyp.8387).
- , and Coauthors, 2015: Integrated modeling of aerosol, cloud, precipitation and land processes at satellite-resolved scales. *Environ. Modell. Software*, **67**, 149–159, doi:[10.1016/j.envsoft.2015.01.007](https://doi.org/10.1016/j.envsoft.2015.01.007).
- Pielke, R. A., R. L. Walko, L. T. Steyaert, P. L. Vidale, G. E. Liston, W. A. Lyons, and T. N. Chase, 1999: The influence of anthropogenic landscape changes on weather in south Florida. *Mon. Wea. Rev.*, **127**, 1663–1673, doi:[10.1175/1520-0493\(1999\)127<1663:TIOALC>2.0.CO;2](https://doi.org/10.1175/1520-0493(1999)127<1663:TIOALC>2.0.CO;2).
- Rasmusson, E. M., 1968: Atmospheric water vapor transport and the water balance of North America. Part II: Large-scale water balance investigations. *Mon. Wea. Rev.*, **96**, 720–734, doi:[10.1175/1520-0493\(1968\)096<0720:AWVTAT>2.0.CO;2](https://doi.org/10.1175/1520-0493(1968)096<0720:AWVTAT>2.0.CO;2).
- , 1971: A study of the hydrology of eastern North America using atmospheric vapor flux data. *Mon. Wea. Rev.*, **99**, 119–135, doi:[10.1175/1520-0493\(1971\)099<0119:ASOTHO>2.3.CO;2](https://doi.org/10.1175/1520-0493(1971)099<0119:ASOTHO>2.3.CO;2).
- Ropelewski, C. F., and M. S. Halpert, 1986: North American precipitation and temperature patterns associated with the El Niño/Southern Oscillation (ENSO). *Mon. Wea. Rev.*, **114**, 2352–2362, doi:[10.1175/1520-0493\(1986\)114<2352:NAPATP>2.0.CO;2](https://doi.org/10.1175/1520-0493(1986)114<2352:NAPATP>2.0.CO;2).
- Rowell, D. P., and C. Blondin, 1990: The influence of soil wetness distribution on short-range rainfall forecasting in the West African Sahel. *Quart. J. Roy. Meteor. Soc.*, **116**, 1471–1485, doi:[10.1002/qj.49711649611](https://doi.org/10.1002/qj.49711649611).
- Santanello, J. A., C. D. Peters-Lidard, and S. V. Kumar, 2011: Diagnosing the sensitivity of local land–atmosphere coupling via the soil moisture–boundary layer interaction. *J. Hydrometeorol.*, **12**, 766–786, doi:[10.1175/JHM-D-10-05014.1](https://doi.org/10.1175/JHM-D-10-05014.1).
- Schubert, S. D., M. J. Suarez, P. J. Pegion, R. D. Koster, and J. T. Bacmeister, 2008: Potential predictability of long-term drought and pluvial conditions in the U.S. Great Plains. *J. Climate*, **21**, 802–816, doi:[10.1175/2007JCLI1741.1](https://doi.org/10.1175/2007JCLI1741.1).
- Seneviratne, S. I., and R. Stöckli, 2008: The role of land–atmosphere interactions for climate variability in Europe. *Climate Variability and Extremes during the Past 100 Years*, S. Brönnimann et al., Eds., Advances in Global Change Research, Vol. 33, Springer, 179–193, doi:[10.1007/978-1-4020-6766-2_12](https://doi.org/10.1007/978-1-4020-6766-2_12).
- , and Coauthors, 2006: Soil moisture memory AGCM simulations: analysis of global land–atmosphere coupling experiment (GLACE) data. *J. Hydrometeorol.*, **7**, 1090–1112, doi:[10.1175/JHM533.1](https://doi.org/10.1175/JHM533.1).
- , and Coauthors, 2013: Impact of soil moisture–climate feedbacks on CMIP5 projections: First results from the GLACE-CMIP5 experiment. *Geophys. Res. Lett.*, **40**, 5212–5217, doi:[10.1002/grl.50956](https://doi.org/10.1002/grl.50956).
- Shukla, J., and Y. Mintz, 1982: The influence of land-surface evapotranspiration on the earth's climate. *Science*, **215**, 1498–1501, doi:[10.1126/science.215.4539.1498](https://doi.org/10.1126/science.215.4539.1498).
- Skamarock, W. C., and J. B. Klemp, 2008: A time-split non-hydrostatic atmospheric model for Weather Research and Forecasting applications. *J. Comput. Phys.*, **227**, 3465–3485, doi:[10.1016/j.jcp.2007.01.037](https://doi.org/10.1016/j.jcp.2007.01.037).
- Tao, W.-K., and Coauthors, 2003: Microphysics, radiation and surface processes in the Goddard Cumulus Ensemble (GCE) model. *Meteor. Atmos. Phys.*, **82**, 97–137.
- Taylor, C. M., and T. Lebel, 1998: Observational evidence of persistent convective-scale rainfall patterns. *Mon. Wea. Rev.*, **126**, 1597–1607, doi:[10.1175/1520-0493\(1998\)126<1597:OEOPCS>2.0.CO;2](https://doi.org/10.1175/1520-0493(1998)126<1597:OEOPCS>2.0.CO;2).
- Ting, M., and H. Wang, 1997: Summertime U.S. precipitation variability and its relation to Pacific sea surface temperature. *J. Climate*, **10**, 1853–1873, doi:[10.1175/1520-0442\(1997\)010<1853:SUSPVA>2.0.CO;2](https://doi.org/10.1175/1520-0442(1997)010<1853:SUSPVA>2.0.CO;2).
- Trenberth, K. E., A. Dai, R. M. Rasmussen, and D. B. Parsons, 2003: The changing character of precipitation. *Bull. Amer. Meteor. Soc.*, **84**, 1205–1217, doi:[10.1175/BAMS-84-9-1205](https://doi.org/10.1175/BAMS-84-9-1205).
- Wang, H., S. Schubert, R. Koster, Y.-G. Ham, and M. Suarez, 2014: On the role of SST forcing in the 2011 and 2012 extreme U.S. heat and drought: A study in contrasts. *J. Hydrometeorol.*, **15**, 1255–1273, doi:[10.1175/JHM-D-13-069.1](https://doi.org/10.1175/JHM-D-13-069.1).
- Weaver, C. P., S. B. Roy, and R. Avissar, 2002: Sensitivity of simulated mesoscale atmospheric circulations resulting from landscape heterogeneity to aspects of model configuration. *J. Geophys. Res.*, **107**, 8041, doi:[10.1029/2001JD000376](https://doi.org/10.1029/2001JD000376).
- Wu, D., C. Peters-Lidard, W.-K. Tao, and W. Peterson, 2016: Evaluation of NU-WRF rainfall forecasts for IFloods. *J. Hydrometeorol.*, **17**, 1317–1335, doi:[10.1175/JHM-D-15-0134.1](https://doi.org/10.1175/JHM-D-15-0134.1).
- Xia, Y., and Coauthors, 2012: Continental-scale water and energy flux analysis and validation for the North American Land Data Assimilation System project phase 2 (NLDAS-2): 1. Intercomparison and application of model products. *J. Geophys. Res.*, **117**, D03109, doi:[10.1029/2011JD016048](https://doi.org/10.1029/2011JD016048).
- Yanai, M., S. Esbensen, and J. H. Chu, 1973: Determination of average bulk properties of tropical cloud clusters from large-scale heat and moisture budgets. *J. Atmos. Sci.*, **30**, 611–627, doi:[10.1175/1520-0469\(1973\)030<0611:DOBPOT>2.0.CO;2](https://doi.org/10.1175/1520-0469(1973)030<0611:DOBPOT>2.0.CO;2).
- Zaitchik, B. F., J. P. Evans, R. A. Geerken, and R. B. Smith, 2007: Climate and vegetation in the Middle East: Interannual variability and drought feedbacks. *J. Climate*, **20**, 3924–3941, doi:[10.1175/JCLI4223.1](https://doi.org/10.1175/JCLI4223.1).
- , J. A. Santanello, S. V. Kumar, and C. D. Peters-Lidard, 2013: Representation of soil moisture feedbacks during drought in NASA Unified WRF (NU-WRF). *J. Hydrometeorol.*, **14**, 360–367, doi:[10.1175/JHM-D-12-069.1](https://doi.org/10.1175/JHM-D-12-069.1).
- Zangvil, A., D. H. Portis, and P. J. Lamb, 2001: Investigation of the large-scale atmospheric moisture field over the midwestern United States in relation to summer precipitation. Part I: Relationships between moisture budget components on different timescales. *J. Climate*, **14**, 582–597, doi:[10.1175/1520-0442\(2001\)014<0582:IOTLSA>2.0.CO;2](https://doi.org/10.1175/1520-0442(2001)014<0582:IOTLSA>2.0.CO;2).
- Zhu, C., R. L. Leung, D. Gochis, Y. Qian, and D. P. Lettenmaier, 2009: Evaluating the influence of antecedent soil moisture on variability of the North American monsoon precipitation in the coupled MM5/VIC modeling system. *J. Adv. Model. Earth Syst.*, **1**, doi:[10.3894/JAMES.2009.1.13](https://doi.org/10.3894/JAMES.2009.1.13).